MONOCHROMATION OF PULSED ELECTRON BEAMS WITH TERAHERTZ RADIATION

C. Abbamonte*, Cornell University (CLASSE), Ithaca, New York, United States
A. Bartnik, J. Maxson, Cornell University, Ithaca, United States

Abstract

Controlling the energy profile of an electron beam is important for continuous and time resolved spectroscopic and imaging applications that require narrow energy spreads. The energy spread of an electron beam is fundamentally limited by the source, but energy spread that is correlated in time or space can be corrected using an appropriate time- and space-varying force. We present a method of reducing energy spread in photo-emitted electron beams in which laser-derived terahertz fields are used to shape the radial and temporal phase spaces. We show analytically and in particle tracking simulations the absolute limits of monochromation that this technique can achieve for a given source, and characterize non-ideal effects that occur at higher frequencies. The interaction is facilitated by a mirror which is reflective to terahertz and largely transmissive to the electron beam, requiring current losses of only a few tens of percent. Our method significantly outperforms the current output of prism-based monochromators while achieving comparable monochromation.

INTRODUCTION

Electron beams with narrow energy spread are essential for high resolution spectroscopy and imaging applications. In particular, electron energy loss spectroscopy (EELS) in electron microscopes can be used to measure chemical composition [1,2], electronic structure [3,4], and atomic bonding environments [5–7]. EELS can also be useful for detecting lattice vibrations (phonons), but such experiments require energy resolutions of a few tens of meV or below. A typical electron monochromator is composed of a prism which disperses the beam followed by an aperture to select out a narrow band of energies, and usually a vast majority of the incident beam is rejected [8]. For the case of an ultrafast electron microscope, in which the charge is already inherently limited by the pulsed beam, a prism-monochromated beam would contain an impractically small amount of signal. For this reason ultrafast EELS has so far been unable to measure low energy-loss signals such as phonons [9–13]. Monochromation that largely preserves beam current is mandatory for obtaining the energy resolution needed for low-loss ultrafast electron spectroscopy.

A promising alternative to prism-based monochromators involves using electromagnetic fields to reduce energy spread by manipulating the energy phase-space of the electron beam. Radiofrequency (rf) cavities are frequently used to improve time resolution in ultrafast experiments by creating a chirp, or energy-time correlation, that focuses the electron pulse in the longitudinal direction [14–16]. In a conjugate manner, the time-space-energy correlations that naturally arise in beam transport can be exploited for precise control of the beam's energy distribution.

We propose a monochromation scheme that uses pulses of terahertz radiation to correct correlated energy spread stored in the longitudinal and transverse degrees of freedom. Interaction between the electrons and a terahertz wave is facilitated by a mirror which is reflective to terahertz radiation but largely transmissive to the electron beam, for example a thin mirror membrane or a wire mesh TEM grid. The general layout we assume is of an electron beam generated from a photocathode in the single electron per pulse limit and so Coulomb interactions are avoided. Electrons are accelerated by a 60 keV dc electron gun, and focused with a solenoid downstream. Our terahertz interaction is tilted mirror scheme, similar to the layout described in [17]. The layout of the beamline is shown in Fig. 1a, the shape of a terahertz pulse is shown in, Fig. 1b, and cartoon of the mirror geometry is shown in Fig. 1c. In Fig. 2 we show an example of particle tracking results, which displays the particle distribution in energy, space, and time for this simulation, and illustrates the overall effect of the monochromator.

CORRELATION BETWEEN ENERGY, POSITION, AND ARRIVAL TIME

The fundamental principle at work is that an electron pulse emitted from a photocathode with vanishing duration and transverse size will have a downstream position and arrival time perfectly correlated with its energy, as higher energy electrons tend to arrive earlier and travel to larger transverse positions. We assume the beam has a finite spread in momentum such that it is a gaussian with standard deviation σ_p in both transverse coordinates, and a forward half-gaussian with standard deviation $\frac{\sigma_p}{\sqrt{2}}$ in the longitudinal direction. At some longitudinal distance Δz down the beamline a particle has transverse position (x, y) and time of arrival t. In the approximations of linear transport, no coupling between x and y, and cylindrically symmetric fields, the final particle coordinates are related to their initial momentum by

$$x = M_{12} p_{x0}, \quad y = M_{12} p_{y0}, \quad t = M_{56} p_{z0}, \qquad (1)$$

where M_{ij} are the components of the 6×6 transport matrix defined in terms of the particle momentum. Defining E_{gun} as the amount of kinetic energy an electron gains inside the dc gun, we now express the final kinetic energy $E = E_{gun} + \frac{1}{2m}(p_{x0}^2 + p_{y0}^2 + p_{z0}^2)$ in terms the final positions:

* cja98@cornell.edu

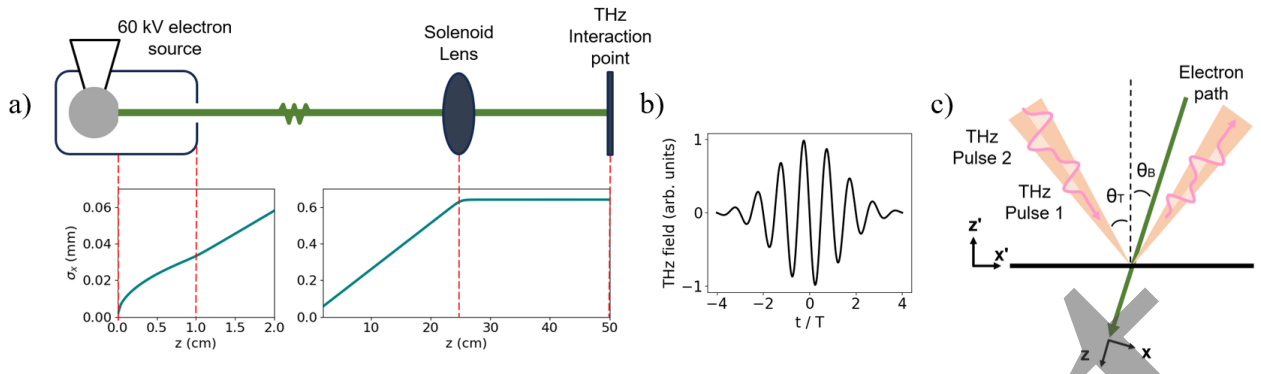

Figure 1: Schematics of the THz monochromator and beamline. ***a)*** Electrons are emitted from a flat photocathode and accelerated by a 60 kV dc gun with a peak field of 6 MV/m and an anode diameter of 3 mm. The beam is collimated in a solenoid before passing through the THz mirror monochromator. ***b)*** The THz pulse shape used for this set of simulations, where t is the time of arrival and T is the period of one cycle. ***c)*** The two THz pulses reflect off of a mirror at angle θ_T to the normal. An electron with zero transverse momentum passes through the mirror at angle θ_B.

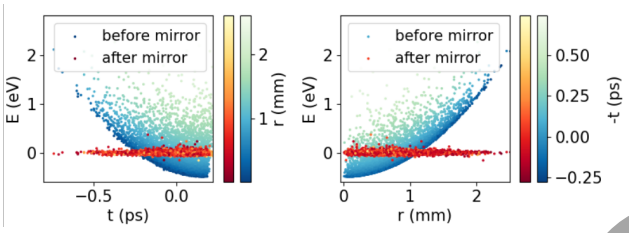

Figure 2: GPT particle distributions before and after the THz monochromator with two pulses at 0.3 THz. Particle energy vs time of arrival colored by radius (left) and particle energy vs radius colored by time of arrival (right).

$$E_{ideal}(r,t) = E_{gun} + \frac{r^2}{2mM_{12}^2} + \frac{t^2}{2mM_{56}^2} \tag{2}$$

where $r = \sqrt{x^2+y^2}$ is the transverse radius, and the subscript on E_{ideal} labels it as the ideal, zero size emitter case. We can see that the energy distribution is a three dimensional paraboloid centered at $x, y, t = 0$. This parabolic energy spread can be seen in the particle tracking simulations that produced the distributions in Fig. 2, where some spreading occurs due to the finite emittance of the beam. The dc gun provides a constant energy boost to every particle, and therefore does not change the energy spread after the point of emission, provided that space-charge effects are negligible.

ANALYTIC MODEL OF ELECTRON BEAM AND TERAHERTZ INTERACTION

Our model is that of a THz pulse incident upon a perfectly reflective mirror, and the electron trajectories are treated as straight line paths through the THz field. The THz pulse is modeled as a gaussian wave packet where E_0 is the amplitude of the electric field at the origin, w_0 is the size of the beam waist, ω_0 is the angular frequency, σ_t is the rms pulse duration, and ϕ_0 is an overall phase offset. The total electric field is the superposition of the incident and reflected THz pulses, each at an angle θ_T relative to the mirror normal. The electron beam passes through the mirror at angle θ_B relative to the mirror normal, with velocity βc, and gains momentum equal to the integral of the force along its trajectory: $\Delta\vec{p} = \int_0^\infty Re\left[\vec{F}_{\text{total}}(x(t), y(t), z(t), t)\right]dt$. Within the approximation of a narrow spectrum ($\omega_0\sigma_t >> 1$), the paraxial limit ($w_0\omega_0/c \gg 1$), and small enough forces to not perturb the electron trajectories, the resulting components of the momentum transfer are,

$$\begin{aligned}\Delta p_z = &\frac{eE_0}{\omega_0} \times \exp\left[\frac{-1}{w_0^2}\left(y^2 + \left(x\frac{\cos\theta_T}{\cos\theta_B}\right)^2\right)\right] \\ &\times \frac{2\cos\theta_B(\beta\sin\theta_B - \sin\theta_T)}{(\beta\cos(\theta_B-\theta_T)-1)(\beta\cos(\theta_B+\theta_T)+1)} \\ &\times \sin\left[\phi_0 - \omega_0\left(t - \frac{x(\beta\sin\theta_T - \sin\theta_B)}{\beta c\cos\theta_B}\right)\right],\end{aligned} \tag{3}$$

and the transverse momentum change Δp_x goes to zero when the angle of incidence is chosen to satisfy $\beta\sin\theta_T = \sin\theta_B$. In this case, we can write the total energy change as $\Delta E = \beta c\Delta p_z$. Taylor expanding ΔE about $(x, y, t) = (0, 0, 0)$ we find that:

$$\Delta E \approx A\left(1 - \frac{r^2}{w_0^2} - \frac{t^2\omega_0^2}{2}\right), \text{for}\,\theta_T \ll 1$$

For small THz incident angles, the energy change evidently takes the form of a negative paraboloid in r and t. Importantly, the coefficients in front of r^2 and t^2 can be tuned independently of one other using the two relevant degrees of freedom for a laser, amplitude and focal size. The curvature in time is determined by the amplitude A (which is proportional to the pulse energy), while the focal size w_0 can be adjisted to match the desired curvature in r. Therefore, to second order, a single THz pulse can perfectly correct energy correlations in an electron beam.

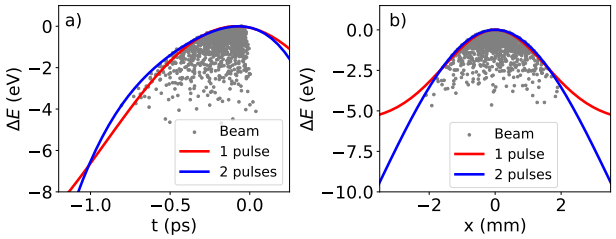

Figure 3: Energy change from 1 pulse (red) and two pulses (blue) for cross sections in **a)** time offset and **b)** radius for a central frequency of 0.3 THz. The gray dots show the negative energy distribution from GPT simulations. The cross sections in time are taken at $(x, y) = 0$, and the cross sections in x are taken at $(y, t) = 0$.

Figure 3 shows the energy change as a function of arrival time and radius for one and two pulses with frequency of 0.3 THz. The parameters E_0 and w_0 were determined based on a numerical minimization of the final energy spread for a simulated distribution of particles. The gray distribution shows the negative energy of the particles, and represents the desired energy change. In other words, maximal monochromation occurs when the curvature of ΔE matches the curvature of the particle energies.

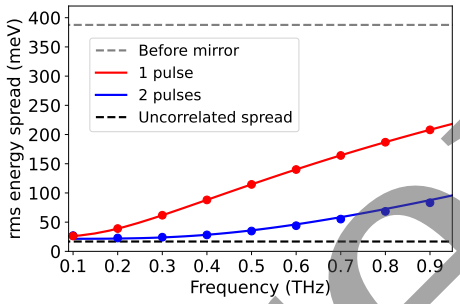

Figure 4: Final energy spread after the THz interaction as a function of THz frequency. The solid lines are found by minimizing σ_E with respect to the parameters E_0 and w_0 in Eq. (3). The points correspond to the result of a GPT simulation using the same parameters.

PARTICLE SIMULATIONS

In this section we describe the particle tracking simulations used to model the THz monochromator, which were performed in General Particle Tracer (GPT) [18]. The GPT simulation consisted of a DC gun at 60 kV, a collimating solenoid, and the THz mirror. The THz pulse and electron beam have angles of incidence θ_T of 20° and θ_B of 5.8° relative to the mirror normal. The initial distribution at the cathode was chosen to resemble that of a realistic state of the art electron source, with a radial size $\sigma_{x0} = 1$ μm and a duration of 30 fs ($\sigma_{t0} = 8.6$ fs).

We modeled the effect of the terahertz mirror on a distribution of particles first by calculating the energy change on each individual particle using the analytic relations described earlier, and second by including the interaction as a custom GPT element with the electric and magnetic fields of a gaussian terahertz wavepacket. We performed a multi-variable numerical minimization on the analytic function (Eq. (3)) to determine the field parameters (pulse energy, width, and time delay) that yielded the smallest energy spread, then used those same parameters for the THz element in GPT. Fig. 4 shows the best final energy spread for one pulse or two pulses as a function of frequency between 0.1 and 1 THz, and demonstrating nearly identical results for the analytic calculations and GPT mirror element.

Table 1: Terahertz Pulse Parameters For Three Frequencies

	0.3 THz	0.6 THz	0.9 THz	Units
Pulse 1: Energy	0.16	2.25	5.14	nJ
Pulse 1: Focal width, rms	0.64	0.81	0.69	mm
Pulse 2: Energy	0.75	3.33	4.55	nJ
Pulse 2: Focal width, rms	0.81	0.83	0.71	mm
Pulse duration, rms	3.33	1.66	1.11	ps
Initial energy spread	0.39	0.39	0.39	V
Final energy spread	**32**	**45**	**74**	**meV**

For one pulse there exists a straightforward optimal combination of parameters at each frequency, while for two pulses the optimization is under-constrained. We find that the final energy spread and pulse energy are competing variables, meaning σ_E can always be made smaller by increasing the energy of the pulses. Conveniently, σ_E asymptotes to its minimum value relatively quickly, and we anticipate that THz energies on the order of tens of nanojoules would be adequate, well within the limit of what current THz generation techniques can achieve. Details on the pulse energy and the optimization parameters are summarized in Table 1.

CONCLUSION

We have shown that laser-derived THz radiation can be used to correct energy spread in an electron beam by exploiting the natural parabolic energy-space correlations that arise from a source with finite momentum spread. We predict that an rms energy spread reduction of more than a factor of ten is possible for a beam with initial energy spread of hundreds of meV, yielding rms energy spreads of a few 10s of meV. We determine through numerical minimization the conditions necessary to correct energy spread correlated with both time and transverse position, and show excellent agreement between our analytic solution and particle tracking simulations. By using a thin membrane or wire mesh as a mirror, the amount of current loss in the electron beam can be limited to a few 10s of percent, thereby significantly outperforming prism-based monochromators in this regard.

ACKNOWLEDGMENTS

This work was supported by DOE awards DE-SC0024907, DE-SC0020144, and the National Science Foundation Grant No. PHY-1549132, the Center for Bright Beams.

REFERENCES

[1] C. Colliex, "Electron energy loss spectroscopy in the electron microscope", in *Advances in Imaging and Electron Physics*,

Elsevier, 2019, pp. 187–304.
doi:10.1016/bs.aiep.2019.04.002

[2] J. A. Hachtel *et al.*, "Identification of site-specific isotopic labels by vibrational spectroscopy in the electron microscope", *Science*, vol. 363, no. 6426, pp. 525–528, Feb. 2019. doi:10.1126/science.aav5845

[3] Y. Sato *et al.*, "High energy-resolution electron energy-loss spectroscopy study of the dielectric properties of bulk and nanoparticle LaB6 in the near-infrared region", *Ultramicroscopy*, vol. 111, no. 8, pp. 1381–1387, Jul. 2011. doi:10.1016/j.ultramic.2011.05.003

[4] M. Terauchi *et al.*, "Performance of a new high-resolution electron energy-loss spectroscopy microscope", *Microscopy Microanalysis Microstructures*, vol. 2, no. 2–3, pp. 351–358, 1991. doi:10.1051/mmm:0199100202-3035100

[5] F. S. Hage *et al.*, "Single-atom vibrational spectroscopy in the scanning transmission electron microscope", *Science*, vol. 367, no. 6482, pp. 1124–1127, Mar. 2020. doi:10.1126/science.aba1136

[6] C. Dwyer *et al.*, "Electron-Beam Mapping of Vibrational Modes with Nanometer Spatial Resolution", *Phys. Rev. Lett.*, vol. 117, no. 25, 2016. doi:10.1103/physrevlett.117.256101

[7] Q. M. Ramasse *et al.*, "Probing the Bonding and Electronic Structure of Single Atom Dopants in Graphene with Electron Energy Loss Spectroscopy", *Nano Letters*, vol. 13, no. 10, pp. 4989–4995, 2013. doi:10.1021/nl304187e

[8] O. L. Krivanek *et al.*, "Vibrational spectroscopy in the electron microscope", *Nature*, vol. 514, no. 7521, pp. 209–212, 2014. doi:10.1038/nature13870

[9] E. Pomarico *et al.*, "meV Resolution in Laser-Assisted Energy-Filtered Transmission Electron Microscopy", *ACS Photonics*, vol. 5, no. 3, pp. 759–764, 2017. doi:10.48550/arXiv.1710.01183

[10] R. K. Li *et al.*, "Femtosecond MeV Electron Energy-Loss Spectroscopy", *Phys. Rev. Appl.*, vol. 8, no. 5, 2017. doi:10.1103/PhysRevApplied.8.054017

[11] I. Madan *et al.*, "Holographic imaging of electromagnetic fields via electron-light quantum interference", *Sci. Adv.*, vol. 5, no. 8, 2019. doi:10.1126/sciadv.aav8358

[12] F. Carbone *et al.*, "EELS femtosecond resolved in 4D ultrafast electron microscopy", *Chem. Phys. Lett.*, vol. 468, no. 4–6, pp. 107–111, 2009. doi:10.1016/j.cplett.2008.12.027

[13] L. Piazza *et al.*, "Simultaneous observation of the quantization and the interference pattern of a plasmonic near-field", *Nat. Commun.*, vol. 6, 2015. doi:10.1038/ncomms7407

[14] R. P. Chatelain *et al.*, "Ultrafast electron diffraction with radio-frequency compressed electron pulses", *Appl. Phys. Lett.*, vol. 101, no. 8, pp. 081901, 2012. doi:10.1063/1.4747155

[15] T. van Oudheusden *et al.*, "Compression of Subrelativistic Space-Charge-Dominated Electron Bunches for Single-Shot Femtosecond Electron Diffraction", *Phys. Rev. Lett.*, vol. 105, no. 26, 2010. doi:10.1103/physrevlett.105.264801

[16] D. Filippetto and H. Qian, "Design of a high-flux instrument for ultrafast electron diffraction and microscopy", *J. Phys. B*, vol. 52, no. 10, 2019. doi:10.1088/0953-4075/49/10/104003

[17] D. Ehberger *et al.*, "Tilted Electron Pulses", *Phys. Rev. Lett.*, vol. 121, no. 9, 2018. doi:10.1103/physrevlett.121.094801

[18] S. B. van der Geer and M. J. de Loos, "General Particle Tracer: A New 3D Code for Accelerator and Beamline Design", in *Proc. EPAC'96*, Sitges, Spain, Jun. 1996, pp. 1241–1243.